SCIENTIFIC REPORTS

OPEN

SUBJECT AREAS:
SOFT MATERIALS
BIOMATERIALS
BIOMATERIALS-PROTEINS
BIOPHYSICS

Received
16 August 2012

Accepted
19 December 2012

Published
24 January 2013

Correspondence and requests for materials should be addressed to P.C. (peggy.cebe@tufts.edu) or C.S. (christoph.schick@uni-rostock.de)

* Current address: Department of Physics & Astronomy, and Department of Biomedical Engineering and Sciences, Rowan University, Glassboro, NJ 08028, USA.

† Current address: Institute for Biomedical Engineering, University of Rostock, 18051 Rostock, Germany.

Beating the Heat - Fast Scanning Melts Silk Beta Sheet Crystals

Peggy Cebe[1], Xiao Hu[2]*, David L. Kaplan[2], Evgeny Zhuravlev[3], Andreas Wurm[3], Daniela Arbeiter[3†] & Christoph Schick[3]

[1]Department of Physics and Astronomy, Medford MA, 02155, USA, [2]Department of Biomedical Engineering Tufts University, Medford MA, 02155, USA, [3]Institute of Physics, University of Rostock, 18051 Rostock, Germany.

Beta-pleated-sheet crystals are among the most stable of protein secondary structures, and are responsible for the remarkable physical properties of many fibrous proteins, such as silk, or proteins forming plaques as in Alzheimer's disease. Previous thinking, and the accepted paradigm, was that beta-pleated-sheet crystals in the dry solid state were so stable they would not melt upon input of heat energy alone. Here we overturn that assumption and demonstrate that beta-pleated-sheet crystals melt directly from the solid state to become random coils, helices, and turns. We use fast scanning chip calorimetry at 2,000 K/s and report the first reversible thermal melting of protein beta-pleated-sheet crystals, exemplified by silk fibroin. The similarity between thermal melting behavior of lamellar crystals of synthetic polymers and beta-pleated-sheet crystals is confirmed. Significance for controlling beta-pleated-sheet content during thermal processing of biomaterials, as well as towards disease therapies, is envisioned based on these new findings.

Many structural proteins, in the solid state, contain extremely stable beta pleated sheets (**Fig. 1**). These secondary structures are stabilized by inter-chain hydrogen bonding in which every amino acid is laterally bonded twice to its nearest neighbor chain segments. The hydrogen bonds are responsible for the extraordinary physical properties of several natural proteins, like silk noted for its high tensile strength (0.5~1.3 GPa), toughness (6×10^4~16×10^4 J/kg)[1–4], biocompatibility, and biodegradability. They also enable the formation of insoluble beta-pleated-sheet structures in many disease-forming proteins such those that form plaques, as in Alzheimer's disease. The present pioneering insights, which demonstrate the feasibility of thermal melting of beta-pleated-sheets, suggest alternative processing strategies for the class of fibrous proteins, and even possibly for novel disease therapies, related to beta-pleated-sheet forming proteins which could be melted by laser fast heating. This work suggests new ways to thermally process solid proteins into novel material forms, useful for biomaterials. The ability reversibly to change the beta-pleated-sheet crystal content in fibrous proteins by fast thermal treatments will have an impact on many aspects of biomaterial properties that need to be controlled for optimal structure-function relationships, including, e.g., mechanical properties, thin film processing, and controlled drug release behavior. Biological outcomes, related to rates of degradability *in vivo,* and responses of cells to silk material scaffolds both critically depend upon beta-pleated-sheet crystal content[2,5,6]. For example, lower beta-pleated-sheet crystal content results in more rapid rates of remodeling of silk-based biomaterials *in vivo* as well as the response of stem cells grown on these fibrous protein substrates[6,7]. Growth of stem cells could also be directed along a patterned substrate, created by selective melting of beta-pleated-sheet crystals on the substrate. The ability to control this crystal phase transition by a reversible thermal process has potential applications in the fields of soft materials *(e.g.,* ultrathin films, hydrogels, microspheres, nanoparticles, nanofibers, or composites), controlled drug release and delivery, biosensors, biophotonics, nano-biotechnology, and tissue regeneration. Beta-pleated-sheet crystal content is directly correlated, for example, to release kinetics of model compounds or drugs sequestered in silk biomaterials[8].

Previous thinking, and the accepted paradigm, was that unlike helical secondary structures or beta strands which can denature in solution, these beta-pleated-sheet crystals in the dry solid state could not melt upon input of heat energy alone. The fast heating methods employed in the present study prove that even beta-pleated-sheet crystal dominated structural proteins like silk, will thermally melt under the appropriate conditions as sketched in **Fig. 1c** and verified by FTIR spectroscopy.

Here we use silk as an exemplary structural protein. Similar to synthetic polymer lamellar crystals, the biomolecular silk chain undergoes chain folding to form two-dimensional sheets which stack together to form three-

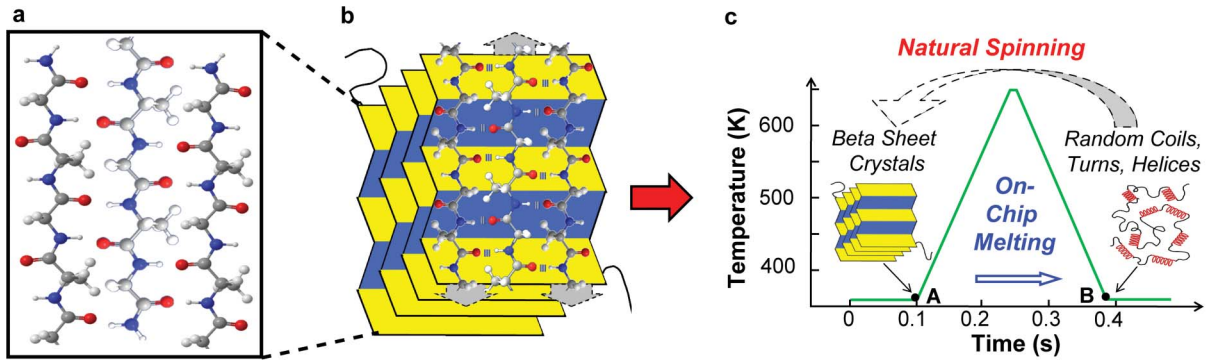

Figure 1 | Silk Fibroin Structure Before and After Assumed Thermal Melting. (a) A three-chain silk sequence is depicted based on the amino acid hexamer, GAGAGS, with anti-parallel molecular chain axes. The chain comprises atoms of carbon (gray), nitrogen (blue), oxygen (red), and hydrogen (white), which have intermolecular hydrogen bonding (represented as three short vertical lines). (b) The molecular chains stack together to form the three-dimensional, beta pleated sheet crystal. This secondary structure is formed by spiders and silkworms naturally during fiber spinning from the solution state, which process converts random coils, turns, and helices into three-dimensional crystals. (c) The temperature vs. time profile is shown during fast thermal treatment, which causes the beta pleated sheet crystals (at point A) to become melted within a few tenths of a second, reversing the natural fiber spinning process, and restoring the material to the non-crystalline solid state (at point B). The on-chip melting uses heating and cooling rates of thousands of degrees per second.

dimensional crystals (**Fig. 1b**). In the *B. mori* domesticated silkworm, beta-pleated-sheet crystals are induced to form naturally during the process of silk fiber spinning from water solution in the salivary gland[5,9–15]. Silk fibroin protein reconstituted from degummed silk also crystallizes into beta-pleated-sheet crystals from concentrated water solutions, or from the dry state upon exposure of the non-crystalline fibroin to methanol (MeOH) or to hot water vapor[5,9,10]. Once formed, the beta-pleated-sheet crystals stabilize the structure and give silk its unique physical properties. The remarkable strength and stability that makes silk useful in garments and in surgical sutures has also impeded efforts by scientists to study its formation and explain its properties. Attempts to melt the beta pleated sheet crystals that comprise silk[16] have always resulted in decomposition which obscures the melting process (**Fig. 2a**). In order fully to characterize fibrous proteins like silk, knowledge of their thermal behavior is essential. Recently, heat capacity measurements were used to investigate the glass transition (T_g) and crystallization (T_c) processes in silk fibroin[16–18], and showed the similarity of these two transitions

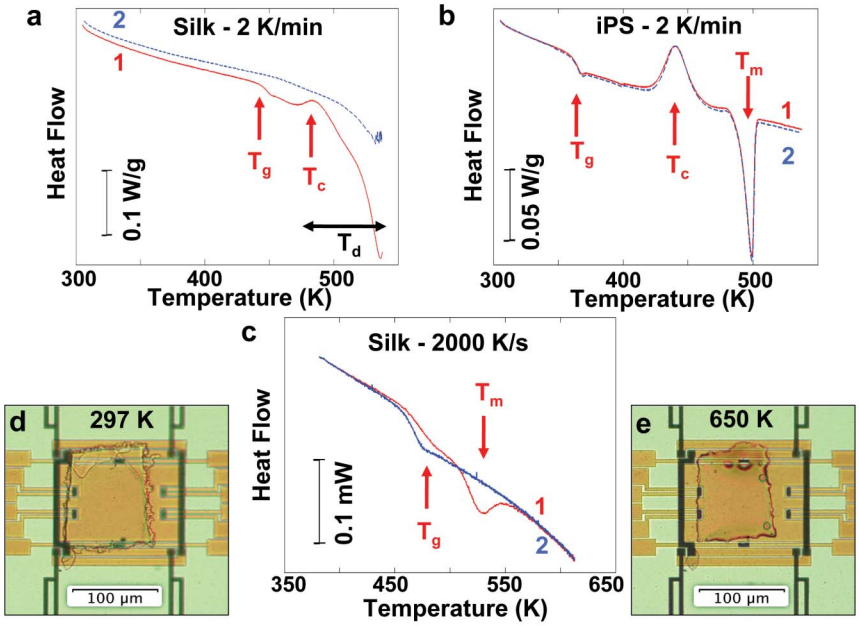

Figure 2 | Comparison of Thermal Characteristics of Silk and Synthetic Polymer at Different Heating Rates. Observable transitions during first (1, red) and second (2, blue) heating include glass transition (T_g), crystallization exotherm (T_c), melting endotherm (T_m), and thermal degradation (T_d). Endotherms are presented with downward deflection. (a) Film of reconstituted *B. mori* silk fibroin protein during DSC heating at 2 K/min. The sample degrades and loses mass upon first heating. The second heating scan does not retrace the first, and no glass transition or crystallization can be observed. (b) Synthetic polymer (exemplified by isotactic polystyrene, iPS) during DSC heating at 2 K/min. Sample does not degrade after heating to 538 K, and the overlapping second heating trace shows the same thermal transitions. (c) Film of reconstituted *B. mori* silk fibroin protein, now heated at 2,000 K/s using fast scanning chip calorimetry, shows melting of beta pleated sheet crystals. The second trace, after cooling from the melt at 2,000 K/s, confirms the non-crystalline nature of the film after beta-pleated-sheets were melted during the first scan. (d, e) Sample from (c), imaged at room temperature with unpolarized light using a 20× objective on the flat, optically transparent sensor, before (d) and after (e) fast heating to 650 K. As a result of melting the film changes shape slightly.

to those seen in flexible-chain synthetic polymers. However, when performing heat flow measurements at the relatively slow rates of 1–20 K/min, typical of differential scanning calorimetry (DSC), the silk melting transition (T_m) is obscured by decomposition[16–18], even though the melting transition is seen in polymers heated under similar conditions. Thermogravimetric studies of silk heated at 2 K/min[12] under nitrogen gas atmosphere showed that thermal decomposition begins at 470 K, and continues to occur over a broad temperature range[7], causing mass loss and converting the silk to black char (**Supplementary Fig. S1**, inset images). Corresponding heat flow data of dry silk (Supplementary Fig. S2, step 4 drying) under nitrogen gas atmosphere (**Fig. 2a**, and **Supplementary Fig. S1**) shows that endothermic heat flow also occurs along with decomposition (signified by T_d). The sample loses 25% of its mass by the time the temperature has reached 548 K (**Supplementary Fig. S1**). In contrast, an unambiguous crystal melting transition occurs in polymers with flexible molecular chains, such as polystyrene (**Fig. 2b**), polyolefins, or nylons. But in silk, beta-pleated-sheet crystal melting cannot be separated from degradation using DSC, even though silk has flexible molecular chains and is a chemical analogue to nylon-2.

The interchain bonding in fibrous proteins is so strong that the intrachain covalent bonds begin to degrade well before the melting transition. As a result, important information about the thermal properties of silk, such as the temperature range of the beta sheet crystal melting, is unable to be assessed using conventional DSC heating rates. It was our thinking that we could mitigate the degradation process, which occurs even under an inert gas environment, by employing a very fast heating rate[19], such as rates now available through use of chip calorimetry (**Fig. 1c**). Then, it would be possible to observe the thermal melting of beta-pleated-sheet crystals and provide fundamental information that would complete the analogy between synthetic polymer thermal transitions and those of fibrous proteins.

Results

The technique of fast scanning chip calorimetry allows a sample to be heated and cooled extremely rapidly, with heating rates[19–21] and also cooling rates[22–25] of many thousands of kelvin per second, providing a temperature vs. time profile illustrated in **Fig. 1c** (see **Supplementary Fig. S2**). In chip calorimetry, time of exposure of a sample to high temperatures is greatly reduced so that an entire heat/cool cycle is completed in ~0.3 s. Through this technology, we obtain heat flow data of proteins within fractions of a second during heating to a very high temperature (>700 K), preventing thermal decomposition that occurs for most proteins at temperatures beginning around ~500 K. This provides us a unique opportunity to investigate the melting behavior of solid protein crystals in the high temperature region (500–700 K).

Thermal analysis of fibroin using fast scanning chip calorimetry is shown in **Fig. 2c** (red curve 1). Silk fibroin containing beta-pleated-sheet crystals, when heated in an inert atmosphere at 2,000 K/s, displays its glass transition at T_g (~474 K, at this heating rate) followed by a complete melting endotherm at T_m (endotherm peak is at ~530 K). Cooling the film at the same fast rate prevents the occurrence of any re-crystallization of the beta-pleated-sheets and a completely non-crystalline sample results (**Fig. 1c**). When this sample is heated a second time (**Fig. 2c**, blue curve 2) the heat flow overlaps the first scan at both low and high temperature. The heat flow trace shows a reduction of T_g (to ~467 K) and a slightly larger step increment at T_g (because there is now more non-crystalline material present) and no melting endotherm (because there are no more beta-pleated-sheet crystals present). Because of the high heating rate also no crystallization is seen (the time the sample is in the temperature range where crystallization can occur is too short). This film was heated and cooled repeatedly at 2,000 K/s, and all subsequent scans overlapped curve 2, indicating that no thermal decomposition has occurred.

The data of **Fig. 2c** were obtained using very small sample masses, on the order of tens of nanograms heated on a chip calorimeter (**Supplementary Fig. S3**). The chip calorimeter contains heating and temperature sensing elements and gives a direct measure of the sample's heat capacity through analysis of the differential power[22–25] (**Supplementary Figs. S3–S7**). All fast scanning experiments are conducted under an inert nitrogen atmosphere. In the center of the chip sensor, the silk film is supported on ~500 nm thin SiN_x membrane covered by a similarly thick SiO_2 layer, which allows infrared radiation to be transmitted through the sample for *in situ* spectroscopic analysis after different stages of thermal treatment. The chain conformation in the crystals yields particular bands in the Fourier transform infrared (FTIR) spectra allowing detection of crystallinity even in these very small samples[16,17,26,27].

The SiN_x membrane is also optically transparent and direct optical imaging of samples was performed before and after fast heating, as shown in **Fig. 2d,e**, respectively. The microscopy was performed at room temperature, *in-situ*, while the sample remained in place on the sensor. Silk fibroin films contained a large fraction, 0.30–0.40[16], of beta-pleated-sheet crystals but nevertheless were optically transparent. This suggests the beta-pleated-sheet crystals are in the nanometer size scale, and therefore do not scatter visible light. Silk fibroin films were found to adhere slightly to the sensor. Visual indication of melting can be seen in smoothing of the cut film edges and some film shrinkage (**Fig. 2d,e**) or forming a droplet out of silk fibers with loss of birefringence (**Figs. 3d,e** and **4a,b**). More importantly, the silk films and fibers after fast heating to 650 K have not been blackened by decomposition.

We used a series of thermal treatments (**Fig. 3**) to demonstrate that melting and crystallization for silk fibroin were fully reversible. The sample was heated and cooled on the chip sensor at 2,000 K/s while heat flow data were collected. Before and after fast heating, the secondary structure of the sample was examined *in-situ* using Fourier transform infrared spectroscopy (FTIR) (**Fig. 3a**)[16] of the spectral regions of Amide I (1600~1700 cm^{-1}, assigned to the peptide backbone) and Amide II (1500–1600 cm^{-1})[26,27]. Secondary structure was correlated with the treatment conditions (**Supplementary Fig. S8**).

First, initially non-crystalline film (**Fig. 3a**, curve M0) contains only helices, turns, random coils and side group secondary structures in Amide I, but no beta-pleated-sheet crystals. In the Amide II region, the Tyrosine ring vibration at 1515 cm^{-1} increases after drying, which we reported previously for thick silk fibroin films[16]. The same sample was then exposed altogether three times to MeOH (by soaking the entire sensor+sample in a vessel containing MeOH and then drying in air) to induce the formation of the beta-pleated-sheet crystals, and each exposure was then immediately followed first by *in situ* FTIR spectroscopy to verify the presence of beta-pleated-sheet crystals and by optical microscopy to document shape and color of the sample, and then by heating at 2,000 K/s in the rapid scan calorimeter to melt the just-formed beta-pleated-sheet crystals. After the rapid calorimetric heating scans the state of the sample was again checked by FTIR spectroscopy and optical microscopy. Without removing the sample from the sensor this cycle was repeated three times.

Absorption spectra after crystallization (*i.e.*, after exposure to MeOH) but before melting (**Fig. 3a**, red curves C1–C3) show the characteristic vibrational band of the antiparallel beta-pleated-sheet crystals at 1629 cm^{-1} [16]. The crystalline sample was then heated to 650 K to melt the crystals, cooled, and examined again with FTIR. Absorption spectra (**Fig. 3a**, blue curves M1–M3) reveal absence of the 1629 cm^{-1} characteristic beta-pleated-sheet vibration, confirming that the silk fibroin beta pleated sheets have been melted by the rapid heating to 650 K, and furthermore, they do not recrystallize upon cooling because of the extremely fast cooling rate. The films are,

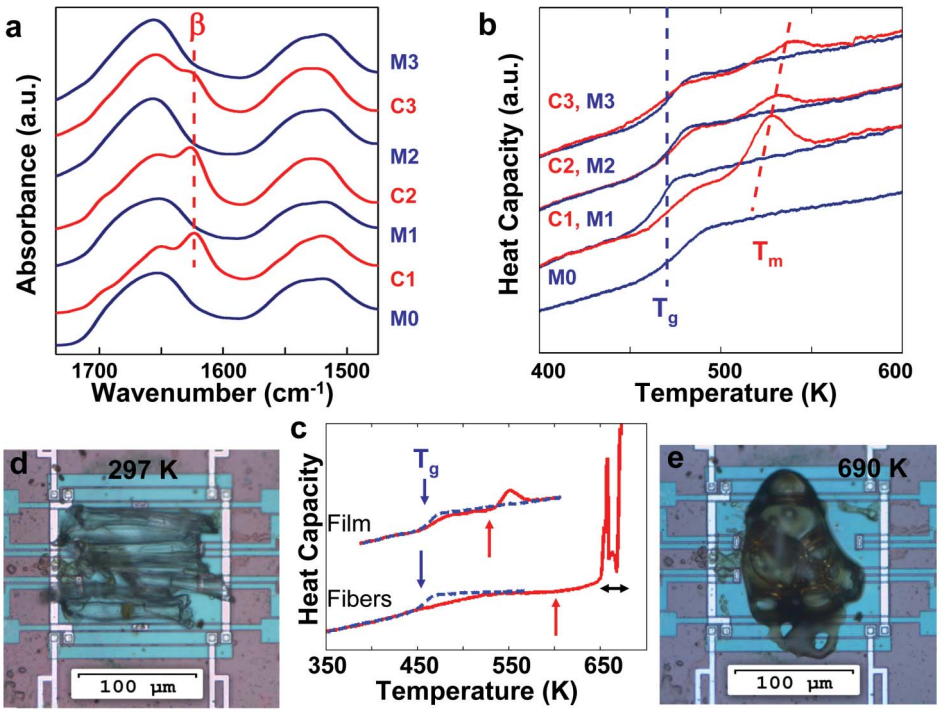

Figure 3 | Comparison of Structural and Fast Scanning Calorimetric Data. Room temperature FTIR absorbance spectra of silk fibroin (a) with corresponding calorimetric data at 2000 K/s (b). (a) Initial non-crystalline silk (M0). Silk exposed in-situ three times to MeOH (C1–C3 red: 18 h – C1; 2.5 h – C2; 20 min – C3) crystallizes, and before fast heating contains beta-pleated-sheet crystals, with characteristic beta sheet absorbance marked at 1629 cm^{-1}. After fast heating to 650 K, beta-pleated-sheet crystals melt and only random coils, turns, and alpha helices remain (M1–M3 blue). (b) Heat capacity vs. temperature at 2000 K/s for the same film shown in (a), presented as matched sets. Initial non-crystalline silk (M0). MeOH-exposed crystalline samples (C1–C3 red) during first heating. After cooling, the film was immediately reheated (M1–M3 blue). Absence of melting endotherms in reheating scans confirms silk is no longer crystalline. (c) Heat capacity vs. temperature at 2000 K/s, for water annealed silk fibroin film and a bundle of native degummed cocoon fibers. Down arrow marks T_g; up arrow marks onset of melting; horizontal black arrow marks region of fiber melting and shape change to droplet morphology. (d, e) A bundle of degummed cocoon fibers, imaged in unpolarized light at 20× magnification before (d) and after (e) heating to 690 K. The separate fibers contract when the beta-pleated-sheet crystals melt, removing the physical crosslinks, and allowing the fibers to coalescence into a single droplet.

however, fully capable of crystallizing once again, either by exposure to MeOH or to hot water vapor (**Fig. 3a**). These exposure treatments result in lowering of the glass transition temperature ("plasticization"), thus providing sufficient mobility to the fibroin molecular chains so that crystallization can occur[17,18]. After exposure, the samples were dried free of water (or MeOH) by heating them above the glass transition temperature (Supplementary Fig. S2, step 4).

Companion thermal scans of this fibroin film taken at 2,000 K/s are shown in **Fig. 3b** for the same set of treatments. Heat capacity traces show the behavior of the initially non-crystalline film (blue curve M0) and then the now-crystalline film after its exposure to MeOH (red curves C1–C3). Each scan of the crystalline film shows a melting endotherm occurring above the glass transition temperature. Superimposed on the first heating scan is a second heating (blue curves M1–M3) showing heat capacity characteristic of non-crystalline material. The second scan displays no melting endotherm, and confirms the FTIR result that no beta-pleated-sheet crystals remain in the fibroin film after melting them in the first heating scan.

Upon rapid cooling at 2,000 K/s to a temperature below the glass transition, the just melted film remains non-crystalline. The cooling and heating rates were sufficiently rapid to prevent recrystallization of molten silk protein during the heat-cool cycle. This behavior is analogous to that of synthetic polymers having glass transition temperatures well above room temperature: (*e.g.,* poly(etheretherketone), PEEK, T_g = 418 K (145°C)[28]; isotactic polystyrene, iPS, T_g = 373 K (100°C)[29]: cooling from the molten state prevents the polymer from crystallizing even at the relatively slower rates of 10–20 K/min used in commercial differential scanning calorimeters. Similarly for silk fibroin protein, the second, and any subsequent, measuring cycles at 2,000 K/s showed the characteristics of a non-crystalline sample: the only feature observed in the heat capacity trace is the well-pronounced glass transition step change. No thermal decomposition peak was observed in the heat capacity, and as a result of the absence of decomposition, the subsequent scans all overlapped each other. The thermal data demonstrate for the first time that the beta-pleated-sheet crystals in silk fibroin films can be reversibly crystallized and thermally melted, and the melting temperature range is from 510–560 K.

The fast heating technique was also applied to a small bundle of degummed native cocoon silk fibers, heating them at 2000 K/s (**Fig. 3c**). (Optical images of a fiber bundle are shown in **Fig. 3d,e** and for a single fiber in **Fig. 4**). The onset of melting of the native fibers occurs at a much higher temperature (~610 K) than the onset of melting of a solvent crystallized silk fibroin protein film (~530 K), regardless of whether the film was water-annealed (**Fig. 3c**) or MeOH treated (**Fig. 3b**). At the same time that beta-pleated-sheet crystals are melting, the highly oriented fibers in the bundle undergo molecular retraction. The reason for the retraction is that the beta-pleated-sheet crystals act as thermo-reversible crosslinks in the fiber. Once the crystals melt, the fiber is able to retract from its as-spun aligned condition, into random coil conformation and a single molten droplet forms (**Fig. 3e**, **Fig. 4b**).

Before melting, FTIR shows that the degummed cocoon fiber comprises highly oriented beta-pleated-sheet crystals (degree of crystallinity ~0.62–0.65[30]). As is typical of oriented crystalline fibers, the

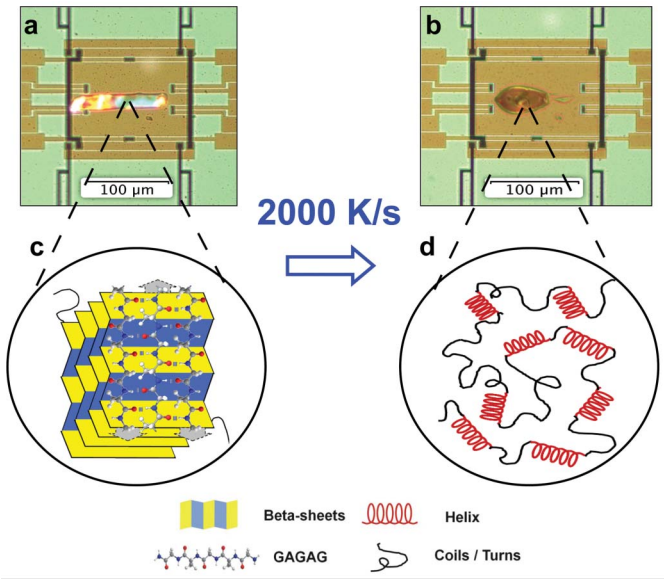

Figure 4 | Silk Structure Before and After Melting. A single degummed native cocoon fiber before (a) and after (b) melting at 2000 K/s, imaged between the polarizer (vertical) and the analyzer (80 degrees to the polarizer) at 10× magnification. Suggested secondary structure is indicated in the lower panels: beta-pleated-sheet crystals in degummed native cocoon fiber (c) and random coils, turns and alpha helices after melting (d). The figure demonstrates the main results of this work, that silk can be melted directly from the solid state upon the input of heat energy alone, without degradation.

polarizing microscope image **Fig. 4a** shows a bright and colorful fiber due to the strongly uniaxial birefringence. That is, the index of refraction of the molecular chains is preferentially aligned along the fiber axis. Upon initial heating to ~690 K, the beta-pleated-sheet crystals in the fiber melt and the fiber loses its orientation (**Fig. 4b**), and hence its birefringence.

Discussion

The findings from this new work have two major implications. First, since the earliest reports of beta-pleated-sheet structures[31] there have been no reported observations of thermally induced melting of dry, solid state beta-pleated-sheet crystals. The fast heating methods employed in the present study prove that even beta-pleated-sheet crystal dominated structural proteins like silk, will thermally melt under the appropriate conditions.

One goal of our research in exploring protein melting phenomenon is to provide a "bridge" between modern synthetic polymer science and biomaterial science, which will benefit multiple scientific areas and broaden interdisciplinary interactions. The second major implication of this work, relating to this goal, is that proteins are analogous to synthetic polymers, even from a thermodynamics perspective. Melting phenomena demonstrate that crystallized solid proteins, exemplified here with silk fibroin, can be considered as fully compatible with all modern polymer theories and experiments about crystallization and melting developed in the last century, with proteins expressing the same thermal transitions as the synthetic polymers, and unfolding from the solid state crystal to the liquid melt through the input of heat energy only. For the first time, we are able to make a direct parallel correspondence between the thermal behavior of protein beta-pleated-sheet crystals, and lamellar crystals of synthetic polymers, identifying the crystal melting transition in addition to the non-crystalline glass transition in both systems. While proteins may be more complex in terms of chemical diversity, with 20 different monomers (amino acids) available in the main chain, previously only aqueous or organic solvent-based processing of such beta-pleated-sheet crystal dominated proteins could be used to understand and control crystallization behavior. With the findings reported here, now thermal processing can also be considered as a processing approach. This finding removes a key distinction between biologically-derived vs. synthetic polymers and allows new thinking about materials engineering even from beta-pleated-sheet crystal enriched structural proteins.

Silks are the prototypical beta-pleated-sheet-containing proteins in nature. Most other proteins utilize beta-pleated-sheets to control protein structure and function, and as such, understanding self-assembly and unfolding of the various structural states and transitions using rapid and controlled thermal heating, would afford new insights into the biophysics and biochemistry of these protein systems. Since reversible thermally-induced melting transitions have been demonstrated for silk, the thermo-analytical methods used in this work can now be applied to any beta-sheet-containing protein, where such secondary structures regulate the stability and function of proteins. The ability to control the beta-sheet structural transitions of proteins in general, via fast scanning calorimetry, could possibly help clarify thermal modes of protein folding and unfolding and optimize the understanding of these transitions. Furthermore, an improved understanding of thermal melting transitions could have broader implications for rules of protein self-assembly, towards protein purification and refolding in the field of biotechnology, for example, or in new ways to think about regulating biocatalysis.

Methods

Materials. Cocoons of *B. mori* silkworm silk (obtained from Tsukuba, Japan), were boiled for 25 min in an aqueous solution of 0.02 M Na_2CO_3 and rinsed thoroughly with water to extract the glue-like sericin[2,7,9,11,16,17,30,32]. The resultant fluffy fibrous material served as the sample for degummed native cocoon silk fibers. To create silk protein films, the silk fibroin protein fibers were dissolved in a 9.3 M LiBr solution at 60°C for 4~6 h, and then dialyzed in distilled water using a Slide-a-Lyzer dialysis cassette (Pierce, MWCO 3500) for 2 days. After centrifugation and filtration to remove insoluble residues, the final 2~5 wt.% silk fibroin aqueous solution was cast in polystyrene Petri dishes to make silk fibroin films. After drying to remove water, the resulting dry film thickness was around 10 μm.

The as-cast films were completely non-crystalline prior to the rapid scan chip calorimetry. Prior to placement on the chip sensor there was no signature of beta pleated sheets in either the FTIR absorption spectrum or the WAXS diffractogram[16]. The dried less ordered, non-crystalline films rapidly and completely dissolved when placed in room temperature water, whereas any semicrystalline films or fibers, containing insoluble beta pleated sheets[7,11,16,17,32,33], would not.

Under an optical microscope, very small pieces of silk fibroin protein film with area typically less than about 100 × 100 μm^2 were cut from the larger parent film. By electrostatic interaction, the film was picked up and placed onto the active area of the chip sensor using a fine wire. The same approach was used to mount individual degummed native cocoon silk fibers, or small bundles of fibers, onto the chip sensor.

Thermal treatments of the samples. Samples of silk fibroin films were subjected to a series of treatments (**Supplementary Fig. S2**) inside or outside the rapid scan calorimeter involving all or some (depending upon sample) of the following steps: 1. erasure of thermal history, 2. crystallization by soaking the entire sensor+sample in a vessel containing MeOH and then drying in air (or by exposure to hot water vapor), 3–4. drying and relaxation, and 5. multiple thermal scans to high temperature at extremely fast rates. All fast scanning was performed under an inert nitrogen gas environment. The degummed native cocoon silk fiber, or small bundles of fibers, were merely dried and thermally scanned (*i.e.,* steps 1 and 2 in **Supplementary Fig. S2** were omitted for the native cocoon silk fibers). During the first measurement cycle to 650 K for silk films (**Supplementary Fig. S2**, first cycle of step 5), all of the crystalline samples containing beta pleated sheet crystals became molten (data shown in **Fig. 3** and **Supplementary Fig. S4**). Upon cooling from the melt to below the glass transition temperature, the samples solidified into non-crystalline films. The second, and all subsequent, measuring cycles showed the samples remained non-crystalline, unless once again subject to crystallizing treatments (**Supplementary Fig. S2**, step 2) which involve exposure to either hot water vapor or methanol (MeOH), or isothermal holding above the glass transition temperature.

Fast Scanning Calorimetry (FSC). The FSC measurements[19–25,34] were performed using a thin film chip sensor XI-399 of Xensor Integration (Netherlands) (**Supplementary Fig. S3**) employing a recently developed differential power compensated calorimeter. Detailed description of the measurement principle and instrumental setup is given elsewhere[22,23]. Due to the small sample mass and small addenda heat capacities, rates as high as 1,000,000 K/s on heating and cooling can be

achieved and heat flow to the sample can be measured up to 100,000 K/s. Two such sensors were connected in a differential scheme with power compensation, as shown in **Supplementary Fig. S4**. One sensor contains the sample; the second one is empty.

After placement of the sample on the sensor and before all measurements a good thermal contact between sensor membrane and sample was established. This usually was done by heating above the glass transition, which enhances sample mobility and allows relaxing, flattening, and adhesion of the sample. Results for an amorphous silk sample for the first and subsequent scans with improved thermal contact are presented in **Supplementary Fig. S6**. The unusual behavior during the first heating scan above 500 K is related to irreversible shape changes of the sample and a resulting improved and stable thermal contact. Coincidence of first and second cooling and the smooth curves verify this. The stable thermal contact of the sample after the first treatment was also not changed after repeated cycles of crystallization and melting (**Fig. 3**).

After crystallization, (**Supplementary Fig. S2**, step 2) a drying step at 430 K (**Supplementary Fig. S2**, step 4), which is below the glass transition (T_g = 451 K[35]), was inserted for removing remaining water. The following relaxation step to 520 K (black curve in **Supplementary Fig. S5**), which is above the glass transition, is necessary for removing the endothermic relaxation peak due to enthalpy relaxation during the drying step 3. The immediate repetition of the latter heating to 520 K (green curve in **Supplementary Fig. S5**) confirms the absence of any enthalpy relaxation peak because of the missing annealing below T_g. In the next heating to 650 K (red curve in **Supplementary Fig. S5**), the melting peak of the beta-pleated-sheets is clearly seen. The repetition of the heating scan to 650 K (blue curve in **Supplementary Fig. S5**) confirms the creation of a non-crystalline sample, as proved by FTIR spectroscopy, by the absence of any endothermic melting peak, and by a more pronounced step at the glass transition, similar to the behavior of synthetic polymers. Further discussion of the chip calorimeter calibration and measurement details are found in **Supplementary Methods**.

Optical microscopy. For morphology studies a Nikon Eclipse E600 Polarizing Optical Microscope (POM) with CCD camera was used. A 10x or 20x long working distance objective lens was used to image silk fibroin samples *in-situ*, while the sample remained in position on the chip sensor. For imaging with unpolarized light (**Figs. 3d,e**), the analyzer and polarizer were set parallel to each other. Imaging with polarized light (**Fig. 2d,e** and **Fig. 4a,b**) was done with the analyzer and polarizer set at 80 degrees to each other. This configuration was used instead of the more customary one (A perpendicular to P) in order to have sufficient light transmission for visual observation and focusing.

Fourier transform infrared spectroscopic analysis. The thin silk fibroin film samples were examined *in situ*, using infrared spectroscopy, with the sample mounted on the chip sensor. Infrared radiation passed through the SiN_x support membrane and the sample was studied in transmission mode using the microscope FTIR spectrometer (Bruker Equinox 55/S) with a liquid nitrogen cooled mercury cadmium telluride (MCT) detector. The position and focus of the samples were adjusted microscopically through an aperture in the IR optical system. The aperture used to give the best signal-to-noise ratio was 10 mm.

For each measurement, 512 scans were co-added and Fourier transformed employing a Genzel-Happ apodization function to yield spectra with a nominal resolution of 4 cm^{-1}. The wave number ranged from 400 to 4000 cm^{-1}. To identify silk secondary structures from the absorption spectra, we obtained the positions of the absorption band maxima from Fourier self-deconvolution[16,36,37] performed by using the Opus 5.0 software[16,37]. To obtain good signal-to-noise ratio, it was required to use relatively thin silk films such as those prepared for use with the chip sensor. This thin film before treatment had no difference in secondary structure when compared with thicker films. Additional details of the Fourier Self Deconvolution process are found in **Supplementary Methods**.

1. Shao, Z. & Vollrath, F. Materials: Surprising strength of silkworm silk. *Nature* **418**, 741–741 (2002).
2. Omenetto, F. G. & Kaplan, D. L. New opportunities for an ancient material. *Science* **329**, 528–531 (2010).
3. Lee, S.-M. *et al.* Greatly increased toughness of infiltrated spider silk. *Science* **324**, 488–492 (2009).
4. Holland, C., Vollrath, F., Ryan, A. J. & Mykhaylyk, O. O. Silk and synthetic polymers: reconciling 100 degrees of separation. *Adv. Mater.* **24**, 105–109 (2012).
5. Altman, G. H. *et al.* Silk-based biomaterials. *Biomater.* **24**, 401–416 (2003).
6. Rockwood, D. N. *et al.* Materials fabrication from Bombyx mori silk fibroin. *Nat. Protocols* **6**, 1612–1631 (2011).
7. Hu, X. *et al.* Regulation of silk material structure by temperature-controlled water vapor annealing. *Biomacromolecules* **12**, 1686–1696 (2011).
8. Pritchard, E. M. & Kaplan, D. L. Silk fibroin biomaterials for controlled release drug delivery. *Expert Opinion on Drug Delivery* **8**, 797–811 (2011).
9. Kaplan, D. L. *et al.* Silk. 103–133, *Protein-Based Materials,* McGrath, K. & Kaplan, D., Eds. (Birkhauser, Boston 1997).
10. Vepari, C. & Kaplan, D. L. Silk as a biomaterial. *Prog. in Polym. Sci.* **32**, 991–1007 (2007).
11. Jin, H.-J. & Kaplan, D. L. Mechanism of silk processing in insects and spiders. *Nature* **424**, 1057–1061 (2003).
12. Zheng, Y. *et al.* Directional water collection on wetted spider silk. *Nature* **463**, 640–643 (2010).
13. Askarieh, G. *et al.* Self-assembly of spider silk proteins is controlled by a pH-sensitive relay. *Nature* **465**, 236–238 (2010).
14. Hagn, F. *et al.* A conserved spider silk domain acts as a molecular switch that controls fibre assembly. *Nature* **465**, 239–242 (2010).
15. Xu, M. & Lewis, R. V. Structure of a protein superfiber: spider dragline silk. *Proc. Natl. Acad. Sci. USA* **87**, 7120–7124 (1990).
16. Hu, X., Kaplan, D. & Cebe, P. Determining beta-sheet crystallinity in fibrous proteins by thermal analysis and infrared spectroscopy. *Macromolecules* **39**, 6161–6170 (2006).
17. Hu, X., Kaplan, D. & Cebe, P. Dynamic protein−water relationships during β-sheet formation. *Macromolecules* **41**, 3939–3948 (2008).
18. Hu, X., Kaplan, D. & Cebe, P. Effect of water on the thermal properties of silk fibroin. *Thermochim. Acta* **461**, 137–144 (2007).
19. Allen, L. H. *et al.* 1000 000 "C/S thin film electrical heater: in situ resistivity measurements of Al and Ti/Si thin films during ultra rapid thermal annealing. *Appl. Phys. Lett.* **64**, 417–419 (1994).
20. Efremov, M. Y. *et al.* Ultrasensitive, fast, thin-film differential scanning calorimeter. *Rev. Sci. Instrum.* **75**, 179–191 (2004).
21. Lopeandia, A. F., Valenzuela, J. & Rodríguez-Viejo, J. Power compensated thin film calorimetry at fast heating rates. *Sensors and Actuators A: Physical* **143**, 256–264 (2008).
22. Zhuravlev, E. & Schick, C. Fast scanning power compensated differential scanning nano-calorimeter: 1. The device. *Thermochim. Acta* **505**, 1–13 (2010).
23. Zhuravlev, E. & Schick, C. Fast scanning power compensated differential scanning nano-calorimeter: 2. Heat capacity analysis. *Thermochim. Acta* **505**, 14–21 (2010).
24. Minakov, A. A. & Schick, C. Ultrafast thermal processing and nanocalorimetry at heating and cooling rates up to 1 MK/s. *Rev. Sci. Instr.* **78**, 073902–073910 (2007).
25. Adamovsky, S. A., Minakov, A. A. & Schick, C. Scanning microcalorimetry at high cooling rate. *Thermochim. Acta* **403**, 55–63 (2003).
26. Barth, A. The infrared absorption of amino acid side chains. *Progr. in Biophysics and Molecular Biology* **74**, 141–173 (2000).
27. Barth, A. & Zscherp, C. What vibrations tell about proteins. *Quarterly Rev. of Biophysics* **35**, 369–430 (2002).
28. Cebe, P. & Hong, S. D. Crystallization behaviour of poly(ether-ether-ketone). *Polymer* **27**, 1183–1192 (1986).
29. Minakov, A. A., Mordvintsev, D. A., Tol, R. & Schick, C. Melting and reorganization of the crystalline fraction and relaxation of the rigid amorphous fraction of isotactic polystyrene on fast heating (30,000 K/min). *Thermochim. Acta* **442**, 25–30 (2006).
30. Warwicker, J. O. Comparative studies of fibroins: II. The crystal structures of various fibroins. *J. of Molecular Biology* **2**, 350–362, IN351 (1960).
31. Pauling, L. & Corey, R. B. The pleated sheet, a new layer configuration of polypeptide chains. *Proc. Natl. Acad. Sci. U S A* **37**, 251–256 (1951).
32. Yu, L., Hu, X., Kaplan, D. & Cebe, P. Dielectric relaxation spectroscopy of hydrated and dehydrated silk fibroin cast from aqueous solution. *Biomacromolecules* **11**, 2766–2775 (2010).
33. Hu, X., Kaplan, D., & Cebe, P. Thermal Analysis of Protein-Mettalic Ion Systems. *J. Thermal Anal. Calorim.* **96**, 827–834 (2009).
34. van Herwaarden, A. W. Overview of calorimeter chips for various applications. *Thermochim. Acta* **432**, 192–201 (2005).
35. Pyda, M., Hu, X. & Cebe, P. Heat Capacity of Silk Fibroin Based on the Vibrational Motion of Poly(amino acid)s in the Presence and Absence of Water. *Macromolecules* **41**, 4786–4793 (2008).
36. Goormaghtigh, E., Cabiaux, V. & Ruysschaert, J.-M. Secondary structure and dosage of soluble and membrane proteins by attenuated total reflection Fourier-transform infrared spectroscopy on hydrated films. *Europ. J. of Biochemistry* **193**, 409–420 (1990).
37. Jung, C. Insight into protein structure and protein–ligand recognition by Fourier transform infrared spectroscopy. *J. Molecular Recognition* **13**, 325–351 (2000).

Acknowledgments

The authors acknowledge support from the National Science Foundation and German Academic Exchange Service DAAD; EZ acknowledges a European Union funded Marie Curie EST fellowship (ADVATEC); XH and DK acknowledge NIH P41 Tissue Engineering Resource Center (P41 EB002520).

Author contributions

P.C., X.H., E.Z., A.W. and D.A. performed the experiments and analyzed the data reported herein. P.C., X.H., D.L.K., E.Z., A.W. and C.S. discussed the experiments, and contributed to writing and editing the paper.

Additional information

Supplementary information accompanies this paper at http://www.nature.com/scientificreports

Competing financial interests: The authors declare no competing financial interests.

How to cite this article: Cebe, P. *et al.* Beating the Heat - Fast Scanning Melts Silk Beta Sheet Crystals. *Sci. Rep.* **3**, 1130; DOI:10.1038/srep01130 (2013).